J Mater Sci (2007) 42:3419–3424
DOI 10.1007/s10853-006-1201-6

Microscopic structural evolution in terms of porosity in high-Tc superconductors

Nasr-Eddine Chakri · Abdelaziz Benaldjia · Abdelaziz Amara · Mohamed Rida Benloucif · Mohamed Guerioune

Received: 8 October 2005 / Accepted: 31 October 2006 / Published online: 23 January 2007

Abstract The low critical current densities of high-Tc superconductors materials can be related to the microstructural imperfections such as pores and microcracks, which reduce the effective current carrying cross section.

The present work examines the characterisation of the state of microstructure and its evolution during thermal treatment of $Bi_2Sr_2Ca_1Cu_2O_8$. The dilatometric analysis was used to study the shrinkage mechanism during sintering. The microstructure of the sintered samples was characterised in terms of pores distribution and apparent density. Open porosity was measured by mercury porosimeter.

In order to compare the results, ultrasonic characterisation such as the longitudinal and transverse wave velocities in the ceramic was carried out. From an ultrasonic point of view, these microstructural features act as inhomogeneities and the ultrasonic parameters will depend on the geometrical arrangement of microstructure (pores have an effect both on Young's modulus and attenuation).

Introduction

The last several years have seen the remarkable development of a new class of ceramics that exhibit superconductivity to unprecedently high temperature [1–3]. Because of their interesting properties (critical current density, diamagnetic response, modulus of superconducting ceramics,...), these materials are promising candidate for potentiel applications [4–7]. It is known that these properties are closely dependant on the microsructure state. Several references [8–11] point to many microstructural variables (compositional variation, pore size ditribution,...) having an impact on velocity. The pore fraction seems to be the major microstructural feature affecting ultrasonic velocities [12–14]. The most important characteristics of microstructure are established through densification, microcracks and porosity during sintering. Ultrasonic measurements of elastic constants as a source of information, offer the advantage of being sensitive to densification and microcracks, which influence the fundamental properties of the materials. In other terms, the elastic properties are sensitive to densification and melting. For this, many measurements of the ultrasonic properties both at kHz and MHz frequencies have been made in high Tc superconductors materials [15–18]. The subsequent increase and decrease in E and G (variation of Young's modulus E and shear modulus G) corresponds to elimination of porosity and reflects the varied ratios of the liquid phase [19, 21]; velocities of ultrasonic waves are, also related to the elastic properties of the materials [12]. So, predictions of longitudinal, transverse and Rayleigh wave velocities (called hereafter V_L, V_T and V_R), are essential in ceramics. Several works [22–26] suggest the role of frequencies and coupling liquids in attenuation, which influence the transmission of energy and the image resolution as well as the absorption through the pores during samples scanning.

N.-E. Chakri (✉) · A. Benaldjia · A. Amara · M. R. Benloucif · M. Guerioune
Laboratoire LEREC, Département de Physique, Faculté des Sciences, Université Badji-Mokhtar Annaba, Sidi-Amar, Annaba 23220, Algeria
e-mail: chakrine@yahoo.com

In the present work, we use the acoustic signature $V(Z)$ analysis to determine V_R of high Tc ceramic superconductors $Bi_2Sr_2Ca_1Cu_2O_8$ (called hereafter Bi-2212) sintered by differential dilatometry technique. E and G are, also, reported.

Experimental procedure

The Bi–Sr–Ca–Cu–O oxides samples were prepared from powder reagent of Bi_2O_3, $SrCO_3$, $CaCO_3$ and CuO. All powders have nominal purities greater than 99.98% and the nominal composition Bi–Sr–Ca–Cu = 2.2–1.8–1.0–2.0 were prepared [27]. The appropriate amounts of powders were mixed and grinded using attritor for 2 h in alcohol with ZrO_2 ball as milling media. The slurry was filtered, dried and then calcined in air at 850 °C for 20 h and is uniaxially cold pressed at 2t/cm^2 to form bars up to 5–6 mm length. Dilatometry analysis (Adamel Lhomargy DI24) is carried out in order to study the shrinkage during sintering. The shrinkage mechanism as a function of temperature was measured directly using uniaxially pressed bars with a dilatometry apparatus linked to a microcomputer for data collection; the analysis is made in air. The densities of the samples were measured with a mercury porosimeter (poresizer 9310, micrometrics) and also deduced from direct measurements. The microstructure observation was performed with a scanning electron microscope (JEOL, JSM840).

In a second stage, a theoretical approach using densities of the coupling liquids (water, methanol and mercury) and ultrasonic measurements of V_L and V_T is considered. According to the theoretical approach for porosity developed here, the acoustic signature $V(Z)$ at the frequency of 30 MHz for the earlier coupling liquids is determined. The treatment of $V(Z)$ by FFT (Fast Fourier Transformation) [28] allows to access to V_R , E and G parameters.

Results and discussions

Dilatometric curves as a function of temperatures are shown in Fig. 1. It indicates that the shrinkage starts at 600 °C and increases as the temperature increases. Over 870 °C, the samples were found deformed. This behaviour may correspond to a small amount of liquid phase assisted-sintering. The maximum shrinkage obtained here is 21%, which corresponds to a final density of 84% compared to the theoretical value. Despite such strong shrinkage the relative density is still low; this unusual feature implies that the shrinkage

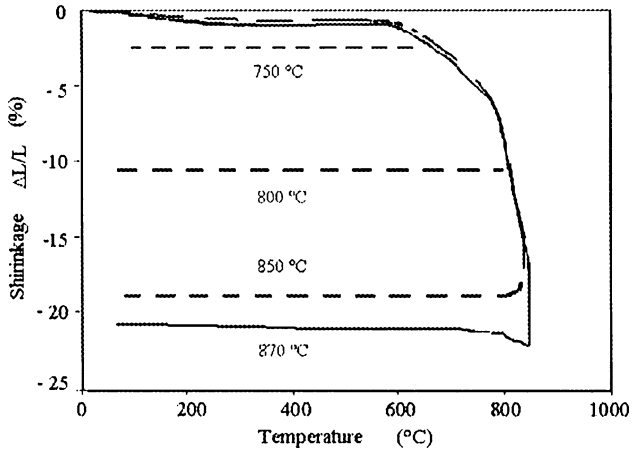

Fig. 1 Dilatometry of Bi-2212 (1h, 2t/cm^2)

is due probably to a thermo-mechanical effect resulting from the applied constant charge during measurement. From this dilatometric experiment we found that a complete densification is far from achieved even with a sintering temperature near the melting point. It is well established [29] that the Bi-based superconductors show a retrograde densification even near the sintering temperature. It is not the case of other superconductor compounds such as YBaCuO. The fracture surface of sintered samples, observed in SEM (see Fig. 2a), shows an important porosity in the temperature range 750–800 °C and the grains start to grow at 800–850 °C, whereas, the porosity is not reduced (see Fig. 2b). At 850–870 °C strong grains are formed and become, more and more, faceted (see Fig. 2c). The anisotropy of the form of grains as plate-like started to develop. From the microstructural point of view, the particle size increases as the sintering temperature increases and remains constant at 870 °C. There is structural evidence indicating that the Bi-2212 phase is made of plate-like grains randomly oriented and distributed. Observations in SEM and density measurements (Table 1) confirmed the microstructural evolution at 750, 800, 850, and 870 °C. The samples sintered in air with 84% of theoretical density exhibit an average grain size of 13 μm. Additionally, the microstructure of sintered samples was characterised in terms of pores distribution (Fig. 3a, b, c). In the ranges of temperature 750–800 °C and 800–850 °C, the pore distribution is centred at 0.4 and 0.2 μm, respectively. At 870 °C, the samples exhibit two populations of pores in the distribution: one is centred at 1.78 μm and another at 32 μm. The large pore distribution is attributed to the microcracks and the creation of open and close porosity, which is amplified by the anisotropy growth of plate-like grains randomly distributed.

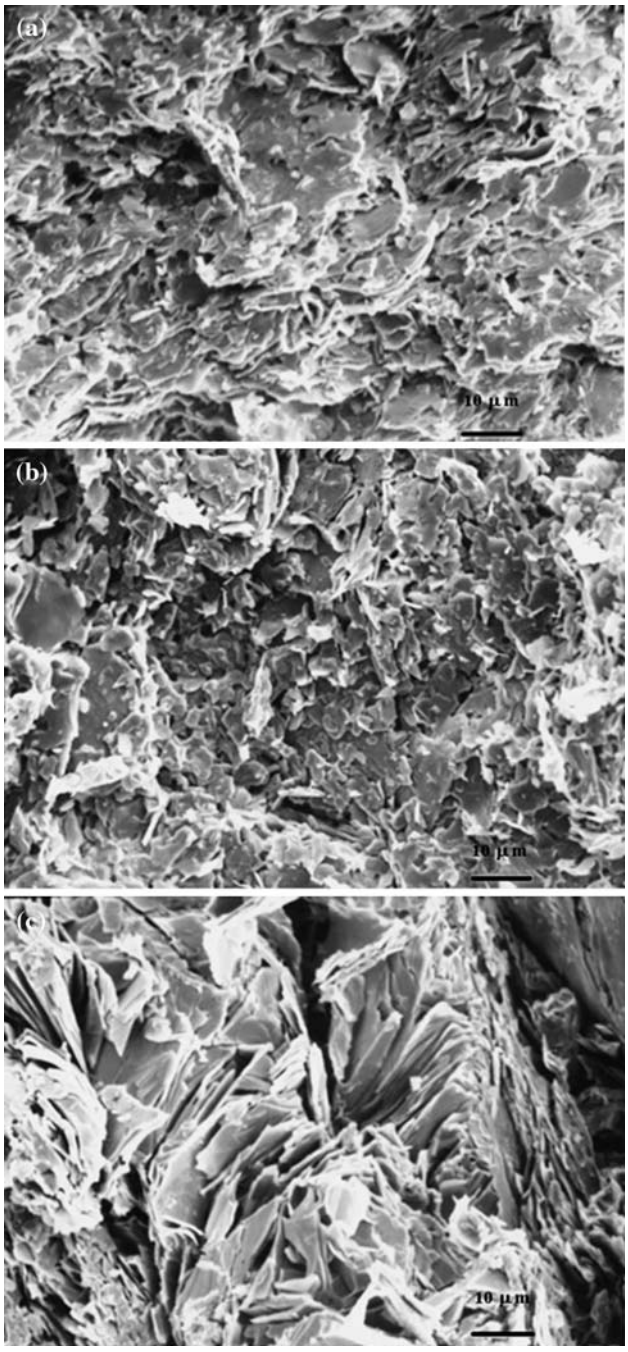

Fig. 2 (**a**) Typical SEM micrograph of samples synthetized at 750–800 °C (**b**) Typical SEM micrograph of samples synthetized at 800–850 °C (**c**) Typical SEM micrograph of samples synthetized at 870 °C

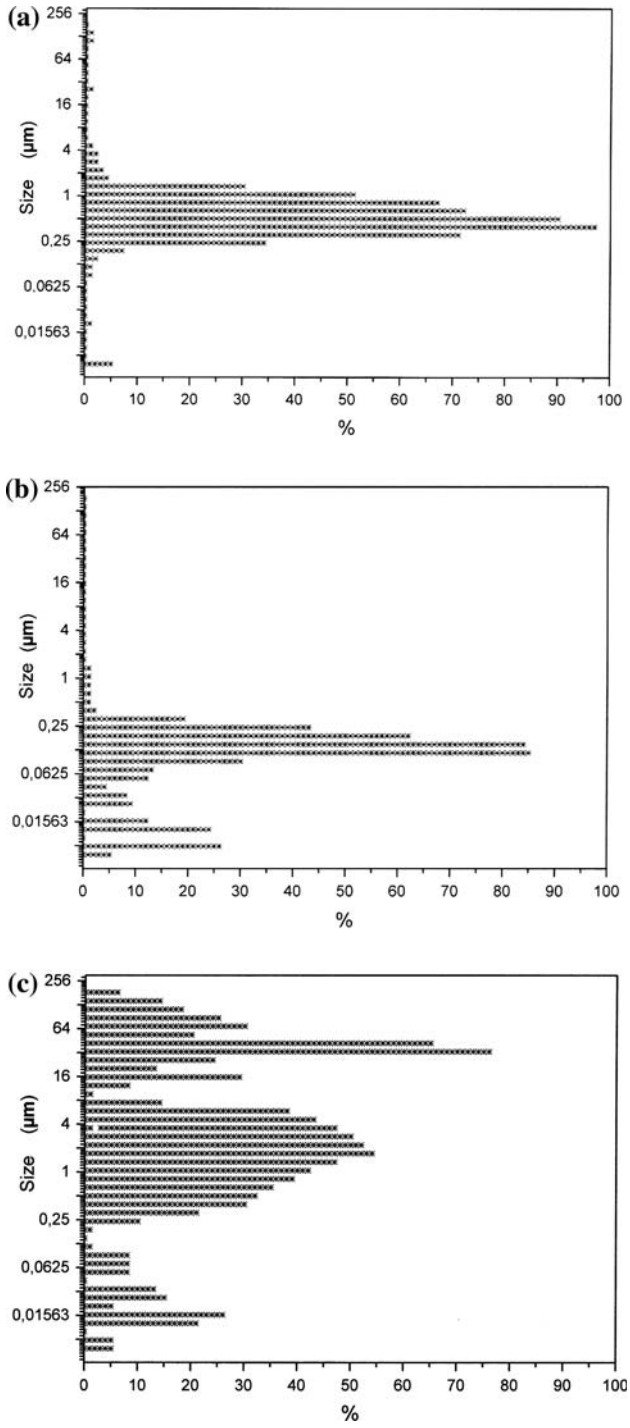

Fig. 3 (**a**) Incremental pore volume vs. pore diameter (at 750–800 °C) (**b**) Incremental pore volume vs. pore diameter (at 800–850 °C) (**c**) Incremental pore volume vs. pore diameter (at 870°C)

Table 1 Variation of density with sintering temperature

T (°C)	750	800	850	870
D_{exp}/D_{th}(%)	70	76	80	84

D_{exp}: experimental density; D_{th}: theoretical density

As the elastic constants and the equivalent wave velocities are closely related to the properties of the Bi-2212 material, an ultrasonic technique is exploited to evaluate the microstructural state. Hence, it is

interesting to study the influence of the coupling liquids (water, methanol and mercury) [26, 30, 31] on the evolution of $V(Z)$ and reflector power $R(\theta)$ at 30 MHz. The principle of $V(Z)$ determination relies on that of acoustic microscopy systems which is based on the emission and reception of ultrasonic waves. In fact, V is the output collected signal by the transducer after having scanned the sample at different defocusing distances Z. The obtained signal has a periodic behaviour; it has been analytically deduced by Sheppard and Wilson model [32] from which the following expression was derived:

$$V(Z) = \int_0^{\pi 2} R(\theta)P^2(\theta)\exp(i2kz\cos\theta)\sin\theta\cos\theta\, d\theta$$

where θ is the angle between a wave vector (k) and the lens axis (Z), $P(\theta)$ is the pupil function of the lens, and $R(\theta)$ is the reflectance function of the specimen. This latter function depends on the coupling liquid—isotropic solid boundary conditions (impedance, density, incidence angle and velocity of different wave modes). The treatment of oscillatory $V(Z)$ curves is carried out via fast Fourier transform, FFT, technique. From the principal ray of these FFT spectra one can deduce the velocity of the most dominant propagating mode [28]. Using classical acoustics, it is easy to determine young's modulus, E, and shear modulus, G, which are functions of longitudinal and transverse velocities.

Moreover, it should be noted that $V(Z)$ signatures are very sensitive to material properties (structural, anisotropy, porosity,...). It has successfully been applied to the investigation of porosity effects on different measured acoustic parameters (longitudinal, transverse, Rayleigh velocities and impedances as well as E and G) of porous silicon [33]. Based on the theoretical values V_L and V_T [12, 16, 30], a program was used to simulate $V(Z)$ and $R(\theta)$ curves. From these curves the different parameters V_R, E and G are extracted (Table 2). One can see clearly the effect of porosity on the above-mentioned parameters; the magnitude of all acoustic parameters decrease as the porosity increases. This behaviour is in agreement with the obtained densities of this synthetised ceramic. It is worth noting that correlations between some ultrasonic parameters and porosity are also reported by previous research [11, 12]. The theoretical $V(Z)$ curves (Fig. 4a–c) show the evolution with different coupling liquids for dense and porous material (20% of porosity). With water as a coupling liquid, the $V(Z)$ attenuation exhibits a periodic aspect in the dense case and is very fast (above 512 μm) for the porous material (Fig. 4a). In the case of methanol, both curves remain periodic with dense and porous material (Fig. 4b). However, when Hg is used, the curves exhibit a perturbation in form of ''flat pseudo-oscillations'' and the attenuation is accentuated for the porous material (Fig. 4c). There is a strong dependence of attenuation on Hg coupling due probably to Hg pressure penetration deficiency into pores and attributed to its surface strains. The behaviour of the simulated $V(Z)$ curves permit to predict if the coupling liquids are absorbed through the pores during scanning samples since they do not influence the velocities. The $V(Z)$ amplitude attenuation is a consequence of the surface microstructure state (pores and grain boundaries) and of the absorption of the coupling liquid which induces, generally, a difference between calculated and measured values.

Conclusion

At lower temperatures the grain size is small and minimises microcracks, whereas at higher temperatures the grain start to grow and their size favours a relatively porous structure with microcrack. During sintering, the appearance of the liquid phase will inhibit the densification process leading to a ''retrograde densification''. The value 90% of theoretical density is not achieved, the material is still porous. It is difficult to predict the porosity distribution and its evolution because at sintering temperature there are several and different pore sizes. The acoustic signature $V(Z)$ determined for our synthesised Bi-2212 material confirm its microstructure state through V_R, E and G values which are in good agreement with dilatometry and porosimetry

Table 2 Values of elastic parameters V_R, E and G corresponding to different coupling liquids

Coupling liquid	*VR* (m/s)		*E* (GPa)		*G* (Gpa)	
	Dense	Porous	Dense	Porous	Dense	Porous
Water (V_L = 1497 m/s)	2620.12	2312.49	119.18	77.42	58.73	37.43
Methanol (V_L = 1103 m/s)	2664.82	2306.05	118.32	73.69	54.80	35.94
Mercury (V_L = 1450 m/s)	2666.62	2309.05	124.65	80.18	60.09	38.84

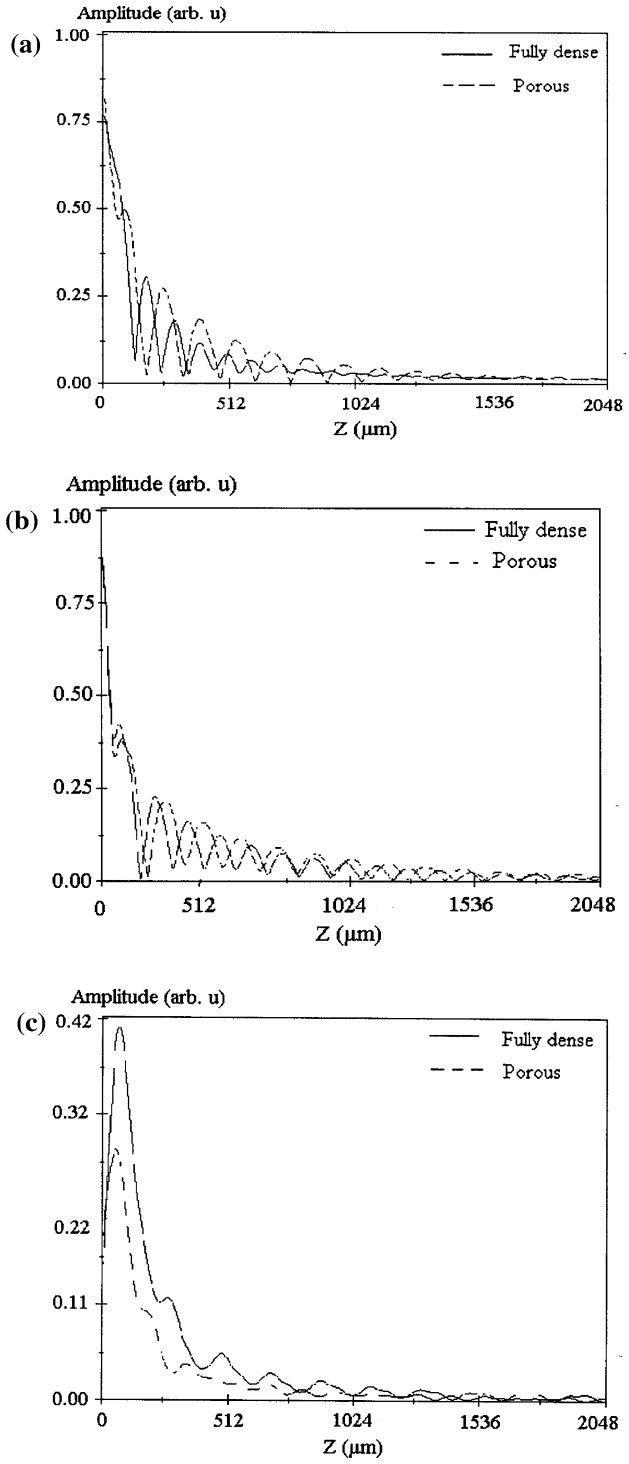

Fig. 4 (**a**) $V(Z)$ acoustic signature of the system water/Bi-2212 at 30 MHz (**b**) $V(Z)$ acoustic signature of the system methanol/Bi-2212 at 30 MHz, (**c**) $V(Z)$ acoustic signature of the system mercury/Bi-2212 at 30 MHz

experiments. The influence of porosity is important on V_R, E and G parameters of the Bi-2212 material. In both methanol and water, the $V(Z)$ curves are periodic and are very suitable for analysis.

V_R, E and G values derived from $V(Z)$ analysis method for Bi-2212 materials (dense or porous materials) are in good agreement with those determined from theoretical expressions.

Our study will be extended to predictions giving for a given porosity an equivalent ultrasonic parameters V_R, E and G. Then, starting from the experimentally obtained V_L, V_R from $V(Z)$ curves, we wish to establish the cartography of porosity fraction evolution (without damaging the samples by the immersion medium). This cartography can be enlarged to other acoustic parameter and allows, consequently, to give any porosity for any measured parameter.

References

1. Bernodz JG, Muller KA (1986) Z Phys B 64:189
2. Chu PH, Hor PH, Meng RL, Gao L, Huang ZJ, Wang YQ, Huang CJ (1987) Phys Rev Lett 58:911
3. Maeda M, Tanaka Y, Fukukum M, Asano T (1988) Jpn J Appl Phys 27:L209
4. Nes OM, Fossheim K, Motolura N, Kitazawa K (1991) Physica C 185–189:1391
5. Wu C-T, Goretta Kc, Poeppel RB (1993) Appl Supercond 1(1/2):33
6. Yasuko Torii, Hirokazu, Hiromi Takei, Kouji Tada (1990) Jpn J Appl Phys 29(6):L 952
7. Guerioune M, Boudour A, Boumaïza Y (1998) congrès Euro méditerranéen. Nantes, France
8. Eva Dresder-Krasicka (1990) Review of Progress in Qualitative N.D.E., vol 9
9. Munro RG (1999) In: Poole CP (ed) Handbook of superconductivity, Academic Press, New York, pp 570–625
10. Alford NMcN, Birchall JD, Clegg WJ, Harmer MA, Kendall K (1988) J Mater Sci 23:761
11. Phani KK, Niyogi SK (1986) J Mater Sci Lett 5:427
12. Blendel JE, Chiang CK, Crammer DC, Freiman SW, Fuller ER Jr, Drescher-Krasicka E, Johnson WL, Ledbetter HM, Bennet LH, Swartzendriber LJ, Marinenko RB, Mykebust RL, Bright DS, Newbery DE (1987) Adv Ceram Mater 2:512
13. Roth DJ, Dolhert LE (1990) Mater Eval 45:958
14. Mukhopadhyay AK, Phani KK (2000) J Eur Ceram Soc 20:29
15. Round R, Bridge B (1987) J Mater Sci Lett 6:1471
16. Dong J, Deng T, Li F, Yao Y (1990) Phys Rev B 42:301
17. Chang F, Ford PJ, Saunders GA, Jiaqiang Li, Almond DP, Chapman B, Cankurtaran M, Poeppel RB, Goretta KC (1993) Supercond Sci Technol 6:484
18. Ravinder Reddy R, Muralidhar M, Hari Babu V, Venugopal Reddy P (1995) Supercond Sci Technol 8:101
19. Reddy PV, Murakami M (1999) Modern Phys Lett B 13(8):261
20. Chandra Sekhar M, Gopala Krishna B, Ravinder Reddy R, Venugopal Reddy P, Suryanarayana SV (1995) Supercond Sci Technol 9:29
21. Ahn Beam-Shu (2002) Bull Korean Chem Soc 23:1304
22. Briggs A (1992) Acoustic microscopy. Clarendon Press, Oxford
23. Ledbetter H, Minglei T, Sudookkim N (1990) Phase Trans 23:61
24. Anderson A, Russel GJ (1991) Physica C 185–189:1389

25. Gigot V, Cros B, Saurel JM (1999) Acta Acoustica 85:346
26. Cros B, Gigot V, Despaux G (1997) Appl Surf Sci 119:242
27. Guerioune M (1994) Thèse Doctorat d'Etat es science, Université de Annaba, pp 52–58
28. Kushibiki J, Chubachi N (1985) Electronic Lett 19(10):359
29. David W, Johonson JR, Warren W. Rodes (1989) J Am Ceram Soc 72(12):2346
30. Tsukahara Y, Neron C, Jen CK, Kushibiki J (1993) Ultrasonic Symposium, 593
31. Brunet N, Cros B, Despaux G, Saurel JM (1998) Eur J Appl Phys 2:209
32. Sheppard CGR, Wilson T (1981) Appl Phys Lett 38:858
33. Boumaiza Y, Hadjoub Z, Doghmane A, Deboub L (1999) J Mat Sc Lett 18:295